Turkish Journal of Physics
http://journals.tubitak.gov.tr/physics/
Research Article

Turk J Phys
(2013) 37: 330 – 347
© TÜBİTAK
doi:10.3906/fiz-1301-4

Structure and odd–even staggering of Mo, Ru, and Pd even–even nuclei in the framework of IBM-1

Vidya DEVI*
Meme Media Laboratory, Hokkaido University, Sapporo, Japan

Received: 07.01.2013 • **Accepted:** 04.07.2013 • **Published Online:** 13.09.2013 • **Printed:** 07.10.2013

Abstract: In this study, we employed the interacting boson model (IBM-1) to determine the most appropriate Hamiltonian for the study of $^{94-108}$Mo, $^{94-110}$Ru, and $^{96-114}$Pd isotopes in the region $A \cong 100$. The soft rotor formula (SRF) calculation was also done to study these isotopes. Using the best fit values of parameters to construct the Hamiltonian of the IBM-1 we calculated energy levels and B(E2) values for number of transitions in Mo, Ru, and Pd nuclei. The results obtained from the IBM-1 and SRF were compared with experimental data and IBM-2 calculation. On comparing the results it was observed that they were in good agreement with each other. The γ-band energy staggering in low-spin, back bending effect, low energy spectra of even–even Mo, Ru, and Pd nuclei is also discussed.

Key words: Interacting boson model (IBM-1), soft rotor formula (SRF), Mo, Ru, Pd isotopes, collectives levels, staggering effect

1. Introduction

The interacting boson model (IBM) model [1, 2, 3, 4, 5] proposed in 1974, is now 40 years old and has undergone many tests [6, 7]. The quantum shape-phase transition as well as the structural evolution of the low-lying states of nuclei can be investigated, as a function of proton and/or neutron number within the framework of an interacting boson model. This kind of analysis has usually been carried out in the IBM-1, in which no distinction is made between proton pairs and neutron pairs. The nuclear shape among which the transitions take place is associated with SU(5), O(6), and SU(3) dynamic symmetries of the IBM-1 model.

A new classification scheme was provided, all nuclei being distributed on the border of a symmetry triangle [8]. The vertices of this triangle symbolize the SU(5) (vibrator), O(6) (γ-soft), and SU(3) (symmetric rotor), while the legs of the triangle denote the transitional region. It was proved that on the SU(5)–O(6) transition leg there exists a critical point for a second order phase transition, while the SU(5)–SU(3) leg has a first order phase transition [9, 10]. It was proved that most nuclei are mapped not on the border of the symmetry triangle but in the interior of the triangle [11, 12]. Examples of such nuclei are the Os and Th isotopes [13, 14]

Iachello [15] pointed out that these critical points correspond to distinct symmetries, namely, E(5) and X(5). For the critical value of an ordering parameter, energies are given by the zeros of a Bessel function of half integer and irrational indices [16, 17, 18]. The X(5) description was extended to the first octupole vibrational band in nuclei close to axial symmetry and also close to the critical point of the SU(5) to SU(3) phase transition [19]. Other symmetries are Y(5) and Z(5) [20, 21]. The former symmetry corresponds to the critical point of

*Correspondence: vidya@nucl.sci.hokudai.ac.jp

the transition from axial to triaxial nuclei, while the latter is related to the critical point of the transition from prolate to oblate through a triaxial shape.

The odd–even staggering (OES) effect observed in the γ-bands is among the most sensitive phenomena carrying information about the symmetry changes. It is quite strongly pronounced in nuclear regions characterized by SU(5) and O(6) and relatively weaker in nuclei near the SU(3) region. In the framework of interacting boson model (IBM), the OES effect has been explained as the result of the interaction between the even angular momentum states of the γ-band and the respective states in the ground state band (gsb) united in the vector boson model with broken SU(3) symmetry [22, 23]. The purpose of this paper is to set some even–even nuclei around the mass region $A \cong 100$. The neutron-rich even–even Mo, Ru, and Pd isotopes around the mass region $A \cong 100$ are very important for understanding the gradual change from a spherical to a deformed state via a transitional phase [24]. We shall also discuss the properties of the IBM-1 and comparison with the IBM-2 and soft rotor formula (SRF).

The outline of the remaining part of this paper is as follow: The theoretical background of IBM-1 is reviewed in Section 2, the E2 and B(E2) transitions are described in Section 2.1, and the soft rotor formula is reviewed in Section 2.2. The calculated energy values and B(E2) values are compared with the experimental and other dynamical symmetries (SU(3), SU(5), O(6), and X(5)) limits in Section 3. We discuss the calculated and experimental γ-band energy staggering pattern as a function of angular momentum in Section 3.1 and the back bending effect in Section 3.2. The last section, Section 4, contains some concluding remarks.

2. The interacting boson model

There are several equivalent ways of writing Hamiltonian H [3]. The most general Hamiltonian that has been used to calculate the level energies is

$$H = \epsilon n_d + a_0 P^{\dagger}.P + a_1 L.L + a_2 Q.Q + a_3 T_3.T_3 + a_4 T_4.T_4 \tag{1}$$

where

$$\begin{aligned}
n_d &= (d^{\dagger}.\tilde{d}), \quad P = \frac{1}{2}(\tilde{d}.\tilde{d}) - \frac{1}{2}(\tilde{s}.\tilde{s}) \\
L &= \sqrt{10}\left[d^{\dagger} \times \tilde{d}\right]^{(1)} \\
Q &= \left[d^{\dagger} \times \tilde{s} + s^{\dagger} \times \tilde{d}\right]^{(2)} - \frac{1}{2}\sqrt{7}\left[d^{\dagger} \times \tilde{d}\right]^{(2)} \\
T_3 &= \left[d^{\dagger} \times \tilde{d}\right]^{(3)}, \quad T_4 = \left[d^{\dagger} \times \tilde{d}\right]^{(4)}.
\end{aligned}$$

Here n_d is the number of operator of d bosons; $s^{\dagger}$, $d^{\dagger}$ and s, d represent the s- and d- boson creation and annihilation operators. Also P, L, Q, T_3, and T_4 in Eq. (1) are the pairing, angular momentum, quadrupole, octopole, and hexadecapole operators, respectively.

The computer program code PHINT [25] was used for the construction of the IBM-1 Hamiltonian and for its solution in the SU(5) basis. The input parameters EPS, PAIR, ELL, QQ, OCT, and HEX are presented in Table 1 related to the coefficients ϵ, a_0, a_1, a_2, a_3, a_4, respectively, $(EPS = \epsilon,\ PAIR = a_0/2,\ ELL = 2a_1,\ QQ = 2a_2,\ OCT = a_3/5,\ HEX = a_4/5)$ [26]. The parameters are free parameters that have been determined so as to reproduce the excitation-energy of all positive parity levels as closely as possible.

Table 1. The best fit values of the Hamiltonian parameters for $^{102-108}$Mo, $^{102-108}$Ru, and $^{104-110}$Pd.

Nuclei	EPS	ELL	QQ	OCT	HEX
^{102}Mo	0.500	–0.350	0.22	0.0011	–2.98504
^{104}Mo	0.400	–0.350	0.22	0.0011	–2.98504
^{106}Mo	0.410	–0.350	0.22	0.0011	–2.98504
^{108}Mo	0.510	–0.300	0.22	0.0011	–2.98504
Nuclei	EPS	ELL	QQ	OCT	HEX
^{102}Ru	0.700	–0.350	0.22	0.0011	–2.98504
^{104}Ru	0.620	–0.400	0.22	0.0011	–2.98504
^{106}Ru	0.600	–0.350	0.22	0.0011	–2.98504
^{108}Ru	0.550	–0.450	0.22	0.0011	–2.98504
Nuclei	EPS	ELL	QQ	OCT	HEX
^{104}Pd	0.800	–0.0350	0.30	0.0010	–2.98504
^{106}Pd	0.650	–0.0300	0.30	0.0010	–2.98504
^{108}Pd	0.600	–0.0310	0.28	0.0010	–2.98504
^{110}Pd	0.500	–0.250	0.30	0.0010	–2.98504

The interacting boson model has a very definite group structure, that of the group U(6). Different reductions of U(6) give 3 dynamical symmetry limits known as harmonic oscillator, deformed rotor, and asymmetric deformed rotor, which are labeled by U(5), SU(3), and O(6), respectively,

$$U(6) \supset U(5) \supset O(5) \supset O(3) \supset O(2)$$

$$U(6) \supset SU(3) \supset O(3) \supset O(2)$$

$$U(6) \supset O(6) \supset O(5) \supset O(3) \supset O(2).$$

The energy eigenvalue for 3 chains are

$$E^{(I)}(N, n_d, \nu, n_\Delta, L, M) = \epsilon n_d + \alpha\frac{1}{2}n_d(n_d-1) + \beta[n_d(n_d+3) - \nu(\nu+3)] + \gamma[L(L+1) - 6n_d]$$

$$E^{(II)}(N, \lambda, \mu, K, L, M) = \left(\frac{3}{4}\kappa - \kappa'\right) L(L+1) - \kappa[\lambda^2 + \mu^2 + \lambda\mu + 3(\lambda+\mu)]$$

$$E^{(III)}(N, \sigma, \tau, \nu_\Delta, L, M) = A\frac{1}{4}(N-\sigma)(N+\sigma+4) + B\frac{1}{6}\tau(\tau+3) + CL(L+1).$$

2.1. The E2 and B(E2) transitions

For the E2 transitions one uses the transition operator T(E2), which is related to the quadrupole operator Q of the Hamiltonian

$$T(E2) = e_b Q = \alpha[d^\dagger s + s^\dagger \tilde{d}]^{(2)} + \beta[d^\dagger \tilde{d}]^{(2)}. \tag{2}$$

Also the charge parameters $\alpha(= e_b)$ and $\beta(= e_b\chi)$ in Eq. (2) are called E2SD and E2DD, respectively. In the consistent Q formalism [27], one uses the same form of the quadrupole operator for the Hamiltonian as well as the T(E2) operator (i.e. the same value of χ). For this, one employs the level energy data as well as the B(E2) values to determine the parameters of H and T(E2). In the alternative procedure, one uses the SU(3) value of χ for the Hamiltonian and the variables α and β (or χ) for the T(E2) operator.

The B(E2) branching ratio for 2 transitions from a particular level in a given band to the 2 states of other band i.e. $(I_i \rightarrow I_f/I_f)$, depends on the Alaga value [28]. In the SU(3) [3] these rules are slightly modified because the $(\gamma \rightarrow g)$ and $(\beta \rightarrow g)$ transitions are prohibited, but in slightly broken symmetry the $(\gamma \rightarrow g)$ transition should be faster than the $(\beta \rightarrow g)$ transition. The observed B(E2) ratios are obtained from the γ-ray spectrum data, using the relation [29]

$$\frac{B(E2; I_i \rightarrow I_f)}{B(E2; I_i \rightarrow I'_f)} = \frac{I_\gamma}{I'_\gamma} \times \frac{(E'_\gamma)^5}{(E_\gamma)^5} \tag{3}$$

where I_γ and I'_γ are the intensities and E_γ and E'_γ are the γ-ray energies for $(I_i \rightarrow I_f)$ and $(I_i \rightarrow I'_f)$ transitions.

2.2. Soft rotor formula (SRF)

Brentano et al. [30] obtained the 2-parameter formula called the soft rotor formula (SRF)

$$E = \frac{J(J+1)}{\alpha(1+\beta J)} \tag{4}$$

The values of α and β are calculated by fitting 2^+_γ, 4^+_γ energies in even sequence and 3^+_γ, 5^+_γ energies in odd sequence. For all these calculations the experimental data are taken from www.nndc.bnl.gov [31].

3. Results and discussion

Figure 1 shows the variation in energy ratio $R_{4/2} = E(4^+_1)/E(2^+_1)$ with neutron number (N) for $^{94-108}$Mo, $^{96-110}$Ru, and $^{100-114}$Pd isotopes. In $^{94-108}$Mo isotopes the $R_{4/2}$ varies from 1.8 to 3.04. These isotopes show the transition from SU(5) to SU(3). In $^{96-110}$Ru the $R_{4/2}$ lies between 1.8 and 2.7 . Hence these nuclei show the transition from vibrational to γ-soft and X(5) critical point. In $^{100-114}$Pd nuclei the $R_{4/2}$ lies from 2.1 to 2.5 and nuclei show transition from vibrational to the γ-soft.

In ^{102}Mo nuclei the 2^+_1 energy is large compared to higher isotopes of Mo. The $R_{4/2}=E(4^+_1)/E(2^+_1)$ value for ^{102}Mo is 2.5, which is close to γ-soft nuclei. The $^{104-108}$Mo nuclei have a low 2^+_1, indicating a large moment of inertia compared to lighter isotopes of the Mo nuclei. The energy ratio $R_{4/2}$ is greater than 2.9, which is near SU(3) values, and so these nuclei may be termed deformed. The quadrupole moment and deformation β_2 for ^{104}Mo [0.33(1)], ^{106}Mo [0.35(1)], ^{108}Mo [0.35(4)] [32] are also large. The calculated band energies in $^{104-108}$Mo are shown in Figures 2 and 3. In ^{104}Mo the calculated values of level energies obtained from IBM-1 and SRF come close to experimental and IBM-2 values. The slopes of g- and γ-bands are almost the same. Thus their dynamic moments of inertia are the same. The rotational structure of the g-band and the γ-band are well given in IBM-1 and SRF calculations. Similarly, good fit to the energies of the g- and γ-band is obtained for ^{106}Mo. The calculated and experimental energy levels are equal. In ^{108}Mo, IBM enables a good fit to the energies of γ-band, but SRF calculation gives good agreement with the experimental values.

In particular, Ru isotopes have recently been investigated within the IBM-1 model [33, 34]. Troltenier et al. [35] also studied the Ru isotopes by using the "geometrical" general collective model (GCM). According to their study the isotopes were found to exhibit spherical structure with a tendency to triaxiality. It is proposed that change in structure is related to experimentally strong neutron–proton interactions. It is also suggested

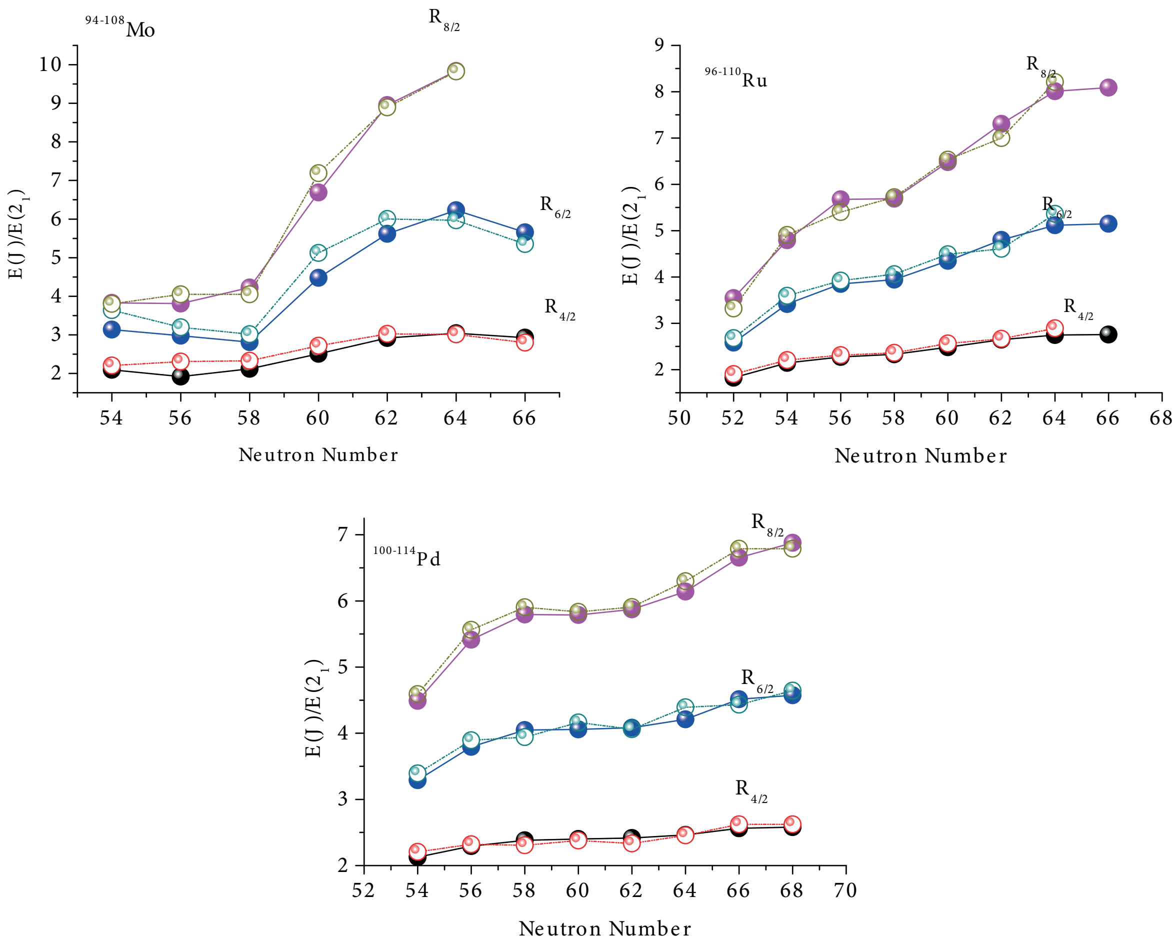

Figure 1. Theoretical (open circle) and experimental (solid circle) energy ratio $E(J)/E(2_1)$ for the $J = 2^+, 4^+, 6^+, 8^+$ levels for even Mo, Ru, and Pd isotopes.

that the neutron–proton effective interactions are of spheriphying nature [36, 37]. The ratio of the energies of the first 4_1^+ and 2_1^+ states is a good criterion for shape transition. The value of $R_{4/2}$ ratio has the limiting value of 2.0 for vibrator, 2.5 for nonaxial γ-soft rotor, and 3.33 for an ideally symmetric rotor. The $R_{4/2}$ ratio increases gradually with neutron number until N = 62 and remains constant for N = 64 and 66. The estimated values change from 2.25 to 2.36. It means that their structure seems to be varying from vibrator to γ-soft. In Figures 4 and 5 we compared the IBM-1 and SRF calculated values with experimental data and IBM-2 calculation. In ^{102}Ru nuclei the $R_{4/2} = 2.32$, which means their structure seems to be varying from vibrator to γ-soft nuclei. There is transition from SU(5) to O(6) symmetry. In these nuclei the g-, γ- and β-band are well produced by IBM-1 and SRF. In ^{104}Ru the $R_{4/2} = 2.48$, which means nuclei are γ-soft in nature. In this case the γ-band is not well generated by IBM-1 but SRF calculations are successful to produce the γ-band. In $^{106-108}$Ru nuclei the $R_{4/2} = 2.6$, 2.7 respectively. Hence structure seems to be varying from γ-soft to the X(5) critical point. The experimental and calculated values show good agreement with each other except for the γ-band in ^{108}Ru nuclei.

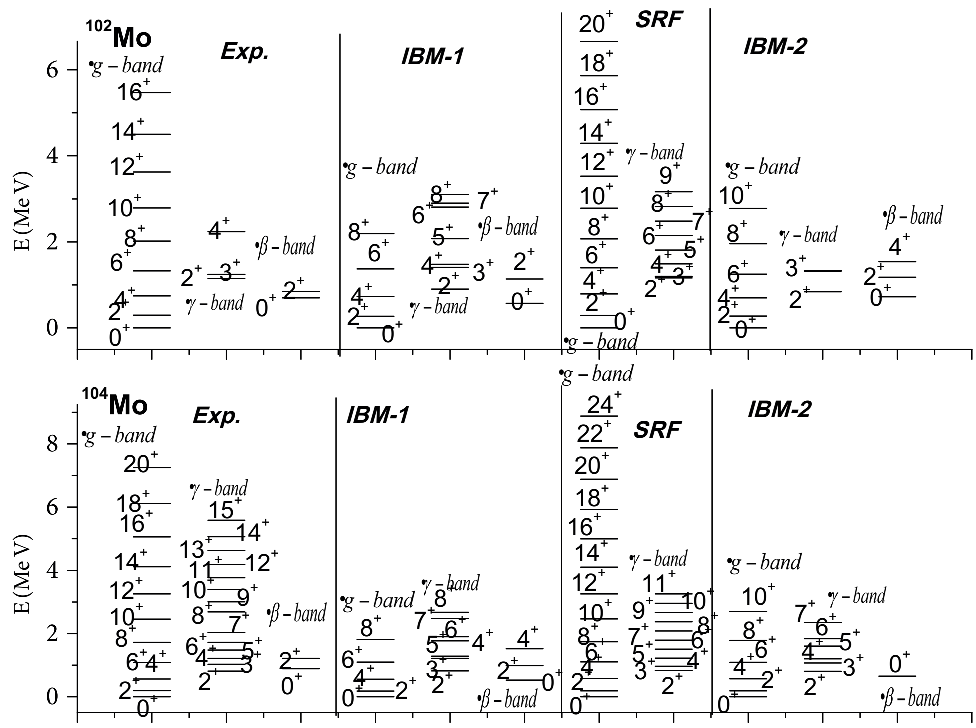

Figure 2. Result of experimental, IBM-1, soft rotor model (SRF), and IBM-2 [42] of ground, quasi-beta, and quasi-gamma band for $^{102-104}$Mo isotopes.

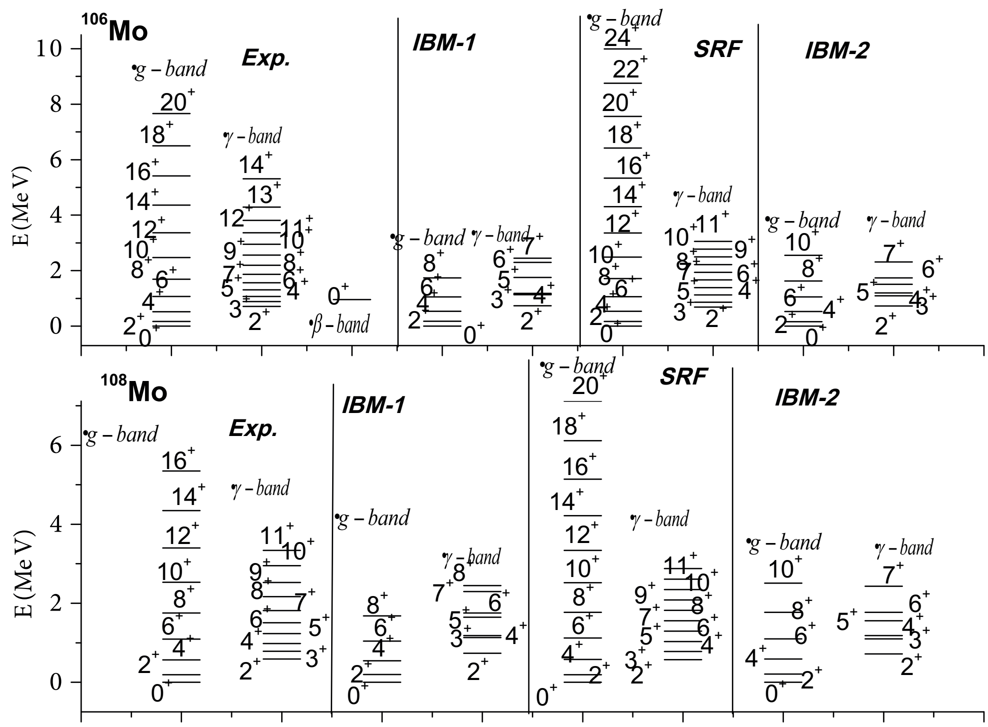

Figure 3. Result of experimental, IBM-1, soft rotor model (SRF), and IBM-2 [42] of ground, quasi-beta, and quasi-gamma band for $^{106-108}$Mo isotopes.

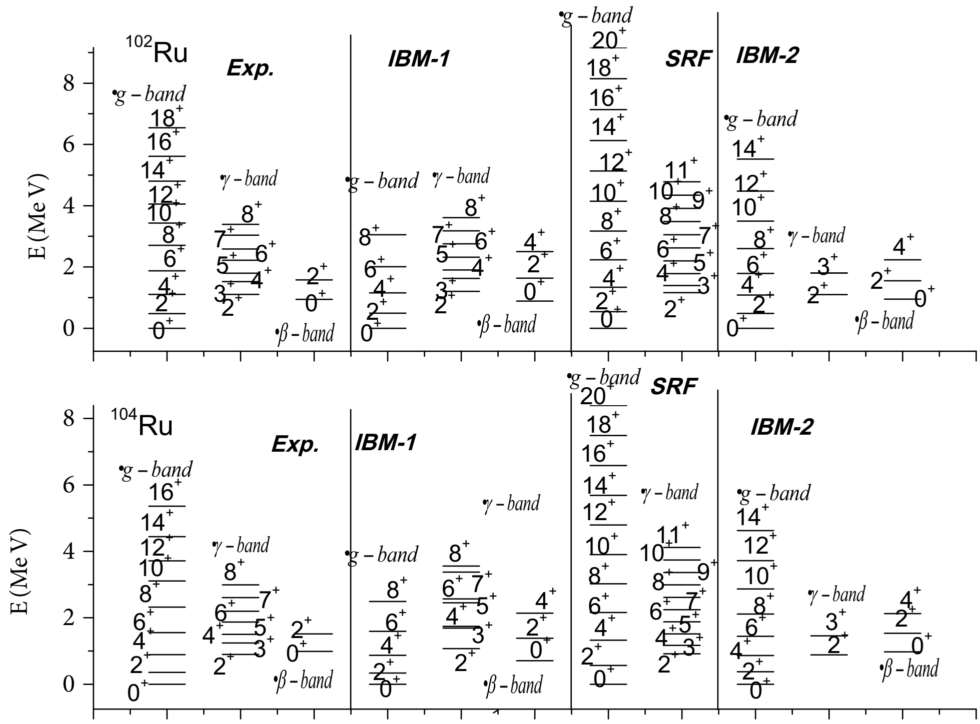

Figure 4. Result of experimental, IBM-1, soft rotor model (SRF), and IBM-2 [43] of ground, quasi-beta, and quasi-gamma band for $^{102-104}$Ru isotopes.

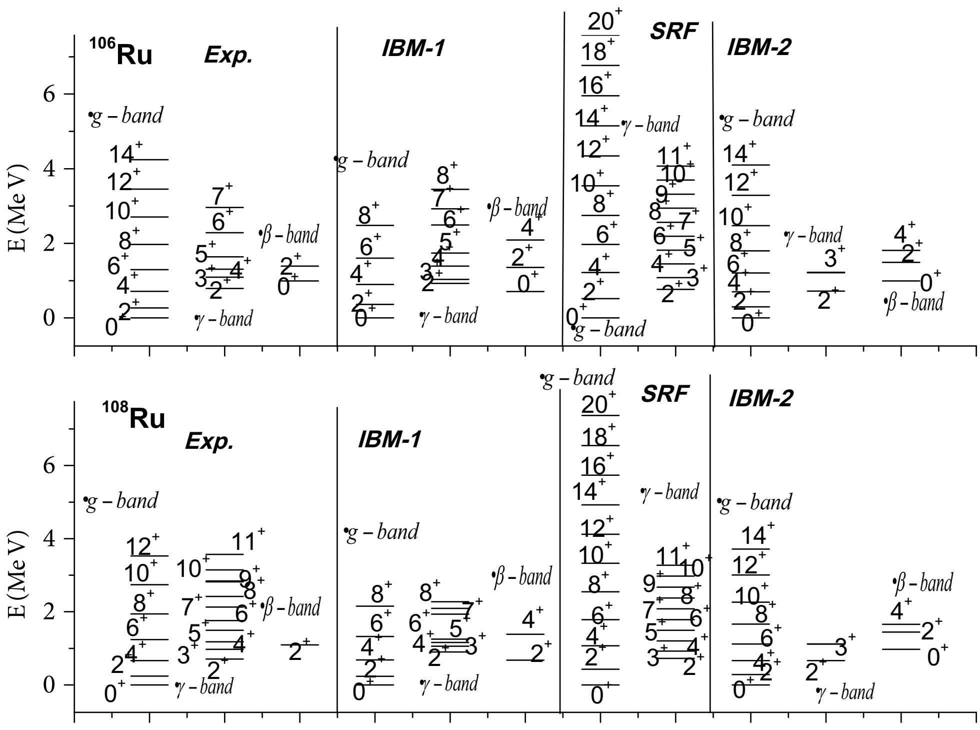

Figure 5. Result of experimental, IBM-1, soft rotor model (SRF), and IBM-2 [43] of ground, quasi-beta, and quasi-gamma band for $^{106-108}$Ru isotopes.

Next Figures 6 and 7 show the comparison of the IBM-1, SRF calculation with experimental and IBM-2 calculation. They show good agreement with each other. Also SRF calculations are successful to calculate some new g- and γ-bands, but not successful in calculating the β-band. The $R_{4/2}$ is 2.4 for $^{104-110}$Pd nuclei. The structure of nuclei seems to be γ-soft in nature.

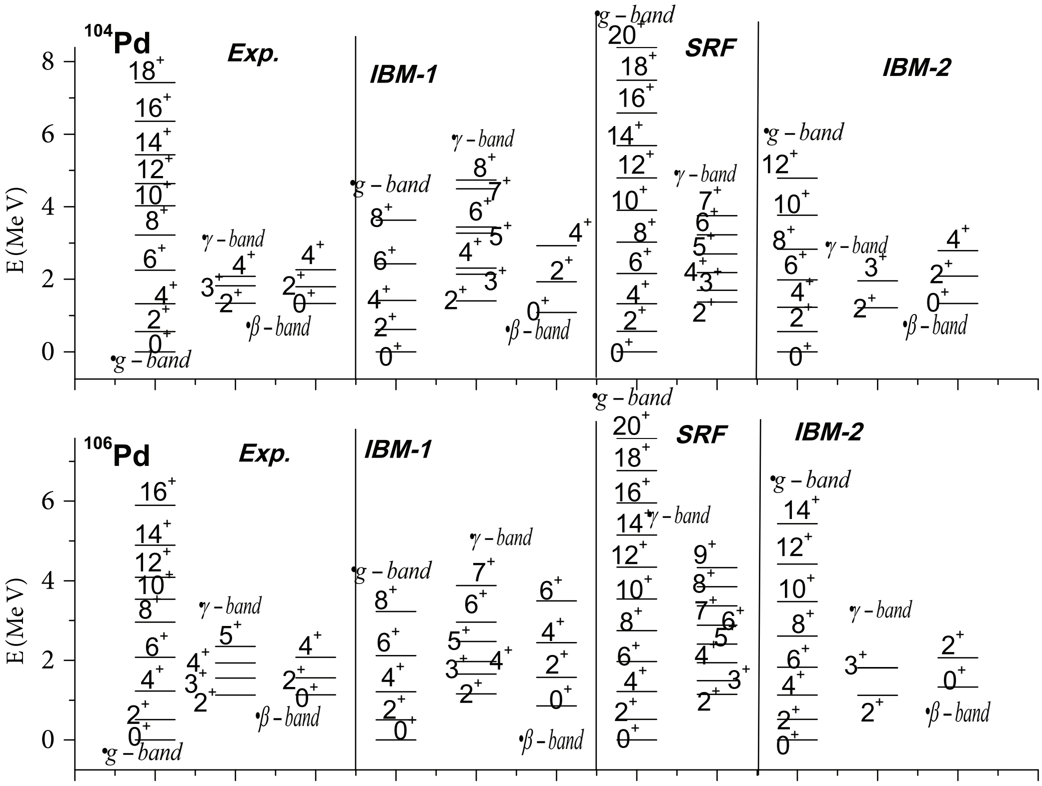

Figure 6. Result of experimental, IBM-1, soft rotor model (SRF), and IBM-2 [44] of ground, quasi-beta, and quasi-gamma band for $^{104-106}$Pd isotopes.

In Figure 8 some B(E2) transition ratios of $^{96-98}$Mo isotopes are given as $R_1 = B(E2; 4_1 \to 2_1)/B(E2; 2_1 \to 0_1)$, $R_2 = B(E2; 2_2 \to 2_1)/B(E2; 2_1 \to 0_1)$, $R_3 = B(E2; 2_2 \to 0_1)/B(E2;\ 2_2 \to 2_1)$ and the calculated ratios are compared with those of SU(5), O(6), SU(3) ratio limits. The results shown in Figure 8 indicate the quality of the fits presented in the paper. In this figure the IBM-1 calculated B(E2) transition ratios are compared with experimental and IBM-2. In most of the cases they show good agreement with the experimental values.

In Figure 9 we present the $B(E2; J \to J-2)$ reduced transitions strength for $^{102-108}$Pd nuclei, which are normalized to their respective $B(E2; J \to J-2)$ values and compared with the expected behavior for an harmonic vibrator, axially deformed rotor, and the X(5) predictions. It is clear from the figure that $^{102-108}$Pd nuclei with yrast energies closely follow the X(5) predictions.

Tables 2 and 3 present some B(E2) (e^2fm^4) transition values for $^{96-100}$Mo, $^{102-104}$Pd, $^{106-110}$Pd, and $^{98-104}$Ru nuclei. These IBM-1 calculated values are compared with the experimental and IBM-2 values. We observed that both formalisms describe fairly well intra-transition in the ground and γ-band. Both calculations show small variation in their B(E2) values but are comparable to the experiment. In the most cases the deviations from the experimental values are smaller than 10%.

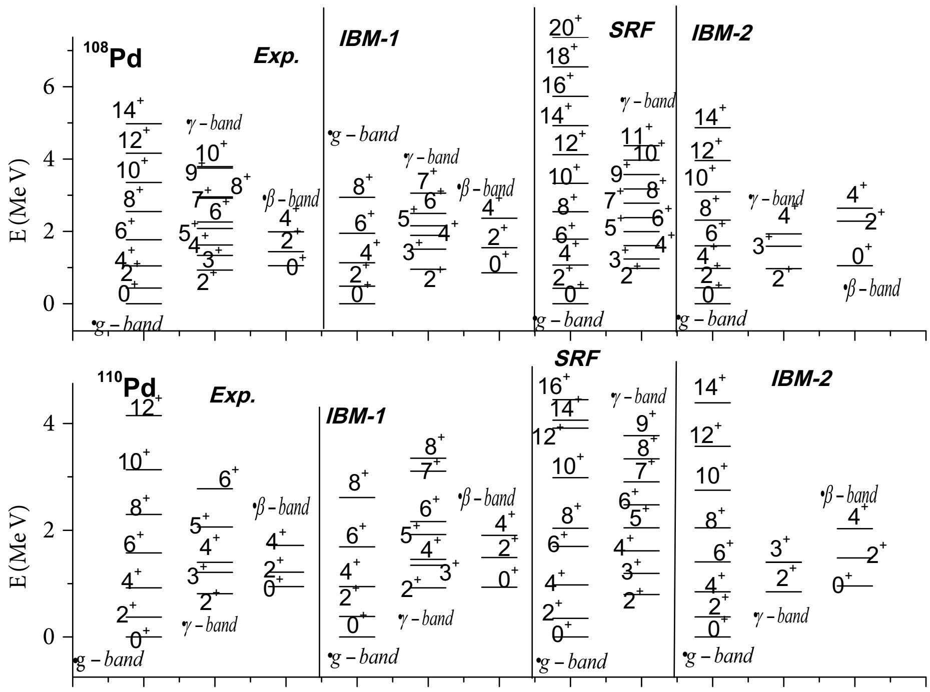

Figure 7. Result of experimental, IBM-1, soft rotor model (SRF), and IBM-2 [44] of ground, quasi-beta, and quasi-gamma band for $^{108-110}$Pd isotopes.7

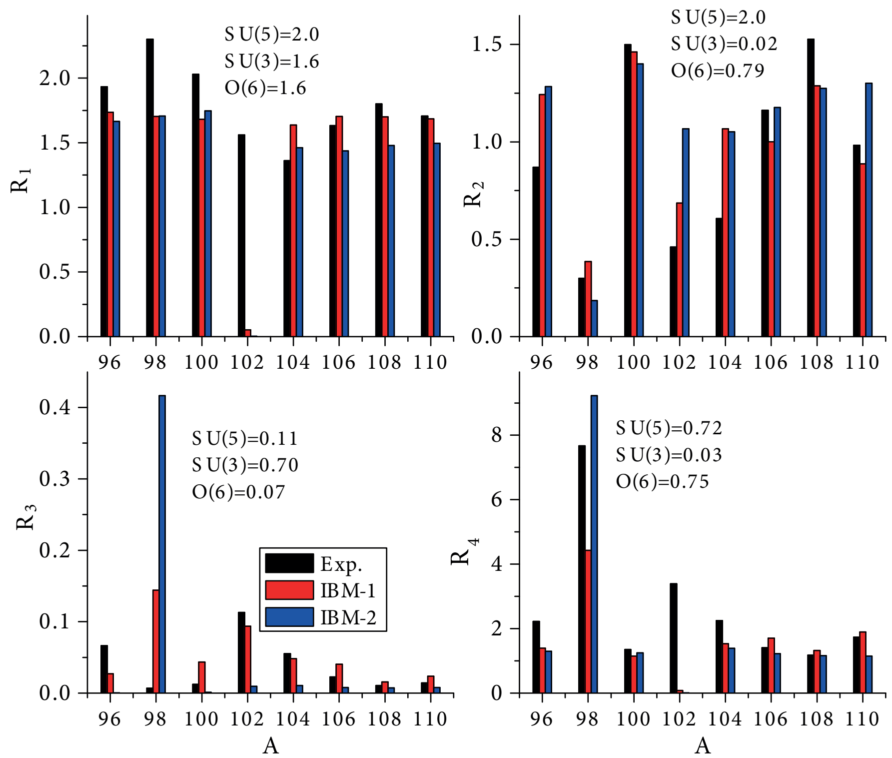

Figure 8. Comparison of systematic of basic observable in Mo, Ru, and Pd isotopes showing $R_1 = B(E2;4_1 \to 2_1)/B(E2;2_1 \to 0_1)$, $R_2 = B(E2;2_2 \to 2_1)/B(E2;2_1 \to 0_1)$, $R_3 = B(E2;2_2 \to 0_1)/B(E2;2_2 \to 2_1)$, and $R_4 = B(E2;4_1 \to 2_1)/B(E2;2_2 \to 2_1)$ ratios of $^{102-108}$Pd isotopes with SU(5), SU(3), and O(6) dynamical symmetry.

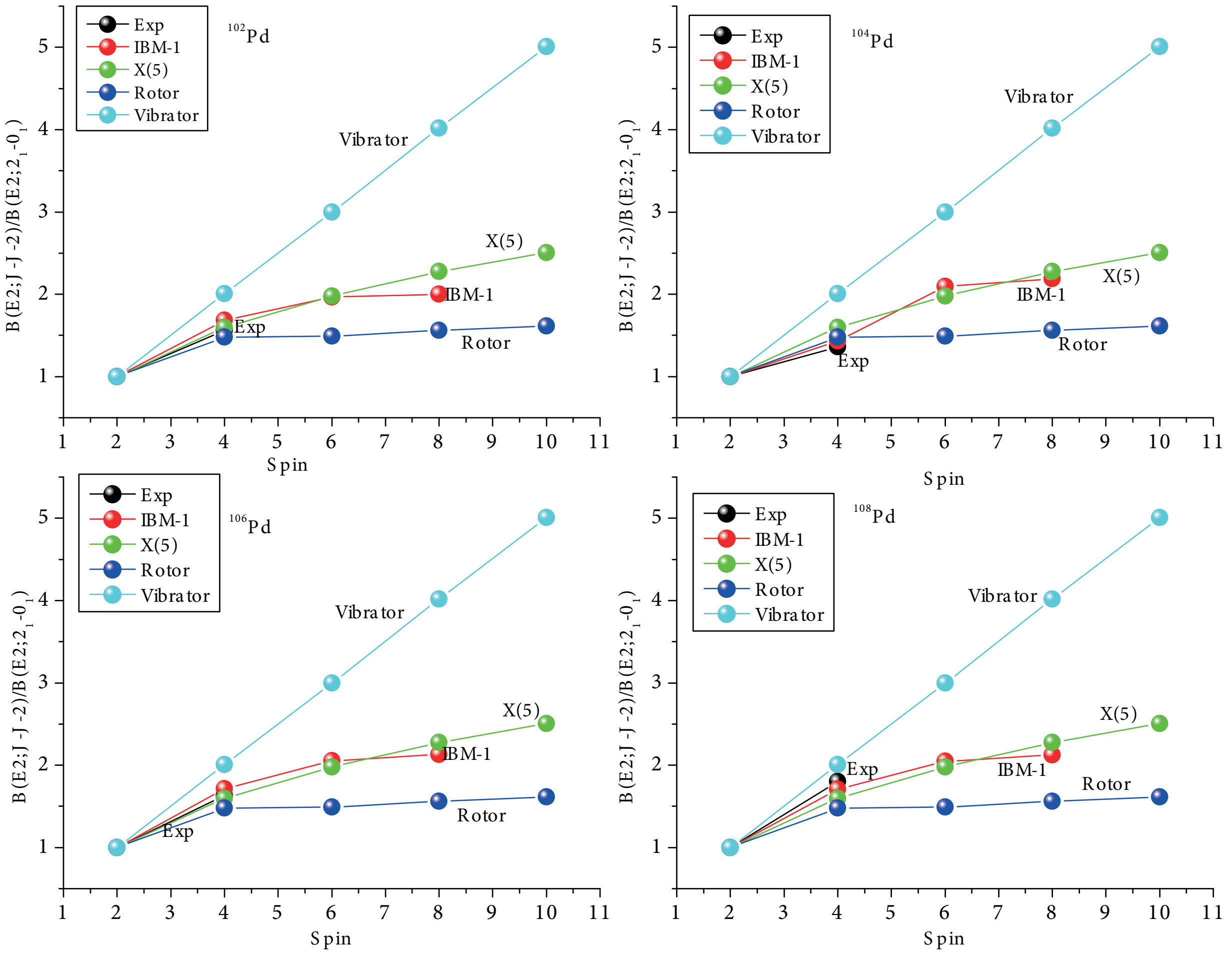

Figure 9. Experimental B(E2) ratios of the g.s. band in $^{102-108}$Pd compared with the predictions of the IBM-1, X(5), rotor, and vibrator limit.

3.1. γ-Band energy staggering patterns as a function of angular momentum

For the study of the staggering effect we consider the following 3-point formula [38]:

$$S(J) = E(J) - \frac{(J+1)E(J-1) + JE(J+1)}{2J+1}, \tag{5}$$

where $E(J)$ denotes the energy of the level with angular momentum J. The odd–even staggering is shown in Figure 10 for $^{104-106}$Mo, ^{104,108}Ru, and ^{108}Pd isotopes. In $^{104-106}$Mo isotopes the observed staggering is generally small as compared to the $^{104-108}$Ru and ^{108}Pd nuclei, as $^{104-106}$Mo nuclei are deformed and staggering is small in SU(3) as compared to O(6) and SU(5). ^{104,108}Ru and ^{108}Pd nuclei show the transition from SU(3) to O(6). Hence odd–even staggering is pronounced with large amplitude. From the above details we deduce that for the considered nuclei the increasing neutron numbers and decreasing proton numbers lead to a systematic suppression of the odd–even staggering effect in the γ-bands. In such a way a region of a better formed rotation structure in these bands is outlined [39].

We used another test of triaxiality on the basis of energy relation $\Delta E_1 = E(3_1^+) - \left[E(2_1^+) + E(2_2^+)\right]$ [14] for triaxial nucleus and $\Delta E_2 = E(3_1^+) - \left[2E(2_1^+) + E(4_1^+)\right]$ for γ-soft nucleus given by Wilets and Jean

Table 2. The experimental and calculated values of BE(2) transitions for $^{96-100}$Mo [42] and $^{102-104}$Pd [45] isotopes.

B(E2)e^2fm^4	Exp.	IBM-1	IBM-2
^{96}**Mo**			
$B(E2;2_1^+\to 0_1^+)$	540.5(7.8)	537.3	543.8
$B(E2;2_2^+\to 0_1^+)$	31.2(2.6)	18	0.2
$B(E2;2_2^+\to 2_1^+)$	470.0(78)	668	698.3
$B(E2;4_1^+\to 2_1^+)$	1044.4(209)	932.2	905.1
$B(E2;4_2^+\to 2_2^+)$	49.6(15.7)	0.096	1.7
$B(E2;4_2^+\to 2_2^+)$	600.5(183)	569.9	125.7
B(E2)e^2fm^4	Exp.	IBM-1	IBM-2
^{98}**Mo**			
$B(E2;2_1^+\to 0_1^+)$	536.8(10.7)	531.6	536.2
$B(E2;2_1^+\to 0_2^+)$	563.6(53.7)	143.5	153
$B(E2;2_3^+\to 0_1^+)$	25.8(1.9)	19	5.9
$B(E2;2_2^+\to 0_1^+)$	1.1(1)	29.5	41.3
$B(E2;2_3^+\to 0_2^+)$	64.4(21.5)	35.8	139.6
$B(E2;2_2^+\to 0_2^+)$	214.7(187.9)	114.7	4.2
$B(E2;2_3^+\to 2_1^+)$	1180.9(107)	998.8	594.6
$B(E2;2_2^+\to 2_1^+)$	161.0(134)	905.4	99.2
$B(E2;4_1^+\to 2_1^+)$	1234.6(134)	905.4	914.9
B(E2)e^2fm^4	Exp.	IBM-1	IBM-2
^{100}**Mo**			
$B(E2;2_1^+\to 0_1^+)$	937.4(55)	935.9	950.2
$B(E2;2_2^+\to 0_1^+)$	17.1(1.4)	59.5	1.3
$B(E2;2_2^+\to 0_2^+)$	151.6(22)	219.6	9.9
$B(E2;2_3^+\to 0_2^+)$	386(110)	465.6	82.6
$B(E2;2_2^+\to 2_1^+)$	1406(137.8)	1367.6	1330.9
$B(E2;2_3^+\to 2_1^+)$	30.9(2.2)	44.7	11.1
$B(E2;2_3^+\to 2_2^+)$	661.7(220.6)	555.3	1.6
$B(E2;4_1^+\to 2_1^+)$	1902.4(110)	1573.3	1659.1
$B(E2;4_2^+\to 2_2^+)$	827.1(165)	933.7	1006.8
$B(E2;4_2^+\to 4_1^+)$	772(165)	668.8	756.1
$B(E2;6_1^+\to 4_1^+)$	2591.7(386)	1837.9	2091.6
$B(E2;8_1^+\to 6_1^+)$	3391.2(496.3)	1877.6	2256.3
B(E2)e^2fm^4	Exp.	IBM-1	IBM-2
^{102}**Pd**			
$B(E2;2_1^+\to 0_1^+)$	923(65)	930.3	899
$B(E2;2_2^+\to 2_1^+)$	425(57)	638.4	959
$B(E2;2_2^+\to 0_1^+)$	48(24)	59.8	9
$B(E2;4_1^+\to 2_1^+)$	1440(71)	1553.5	1225
B(E2)e^2fm^4	Exp.	IBM-1	IBM-2
^{104}**Pd**			
$B(E2;2_1^+\to 0_1^+)$	1045(58)	1046.8	1157
$B(E2;2_2^+\to 2_1^+)$	4633(49)	1117	1211
$B(E2;2_2^+\to 0_1^+)$	35(4)	53.9	13
$B(E2;4_1^+\to 2_1^+)$	1423(203)	1714	1690
$B(E2;2_3^+\to 2_1^+)$	<32	32.1	1

Table 3. The experimental and calculated values of BE(2) transitions for $^{106-110}$Pd [45] and $^{98-104}$Ru[46] isotopes.

B(E2)e^2fm^4	Exp.	IBM-1	IBM-2
^{106}**Pd**			
$B(E2;2_1^+\rightarrow 0_1^+)$	1332(45)	1329.4	1416
$B(E2;2_2^+\rightarrow 2_1^+)$	1548(140)	1330.6	1666
$B(E2;2_2^+\rightarrow 0_1^+)$	35(4)	76.5	14
$B(E2;4_1^+\rightarrow 2_1^+)$	2175(297)	2263.8	2035
B(E2)e^2fm^4	Exp.	IBM-1	IBM-2
^{108}**Pd**			
$B(E2;2_1^+\rightarrow 0_1^+)$	1561(40)	1563.3	1616
$B(E2;2_2^+\rightarrow 2_1^+)$	2383(214)	2012.2	2059
$B(E2;2_2^+\rightarrow 0_1^+)$	25(3)	31.6	13
$B(E2;4_1^+\rightarrow 2_1^+)$	2810(366)	2657	2389
B(E2)e^2fm^4	Exp.	IBM-1	IBM-2
^{110}**Pd**			
$B(E2;2_1^+\rightarrow 0_1^+)$	1711(118)	1714	1869
$B(E2;2_2^+\rightarrow 2_1^+)$	1681(294)	1521.4	2431
$B(E2;2_2^+\rightarrow 0_1^+)$	24(3)	35.9	19
$B(E2;4_1^+\rightarrow 2_1^+)$	2920(383)	2886.3	2795
B(E2)e^2fm^4	Exp.	IBM-1	IBM-2
^{98}**Ru**			
$B(E2;2_1^+\rightarrow 0_1^+)$	78.4(24)	76.2	78.3
$B(E2;4_1^+\rightarrow 2_1^+)$	107.7(122)	105.6	108.8
$B(E2;2_1^+\rightarrow 0_2^+)$		2.6	7.1
$B(E2;2_2^+\rightarrow 0_1^+)$		1.7	0.9
$B(E2;2_2^+\rightarrow 2_1^+)$	147(25)	65.4	39.1
B(E2)e^2fm^4	Exp.	IBM-1	IBM-2
^{100}**Ru**			
$B(E2;2_1^+\rightarrow 0_1^+)$	100.2(2)	107.8	102.2
$B(E2;4_1^+\rightarrow 2_1^+)$	144.4(122)	135.7	143
$B(E2;2_1^+\rightarrow 0_2^+)$		3.4	6.5
$B(E2;2_2^+\rightarrow 0_1^+)$	4.1(46)	3.2	1.5
$B(E2;2_2^+\rightarrow 2_1^+)$	88(13)	76.4	95
B(E2)e^2fm^4	Exp.	IBM-1	IBM-2
^{102}**Ru**			
$B(E2;2_1^+\rightarrow 0_1^+)$	130.2(32)	131.3	130.1
$B(E2;4_1^+\rightarrow 2_1^+)$	211.6(233)	232.5	181.9
$B(E2;2_1^+\rightarrow 0_2^+)$		40.5	3.5
$B(E2;2_2^+\rightarrow 0_1^+)$	4.2(4)	4.4	0.6
$B(E2;2_2^+\rightarrow 2_1^+)$	117(15)	96	160.3
B(E2)e^2fm^4	Exp.	IBM-1	IBM-2
^{104}**Ru**			
$B(E2;2_1^+\rightarrow 0_1^+)$	167.0(9)	163.8	167
$B(E2;4_1^+\rightarrow 2_1^+)$	239(26)	234.9	239
$B(E2;2_1^+\rightarrow 0_2^+)$		24	6
$B(E2;2_2^+\rightarrow 0_1^+)$	0.6	3.6	5
$B(E2;2_2^+\rightarrow 2_1^+)$	167(20)	145.8	147

[40]. In Table 4 we present the experimental and IBM-1 calculated values of ΔE_1 and ΔE_2 for the different isotopes of the $^{94-108}$Mo, $^{96-108}$Ru and $^{100-110}$Pd. In this study we observed that their are some isotopes like ^{106}Mo, ^{108}Mo, ^{104}Ru, and ^{106}Ru), which have ΔE_1=3.2, 3.3, 8.9, and 3.2, respectively. These deviations suggested that these nuclei have some triaxial nature.

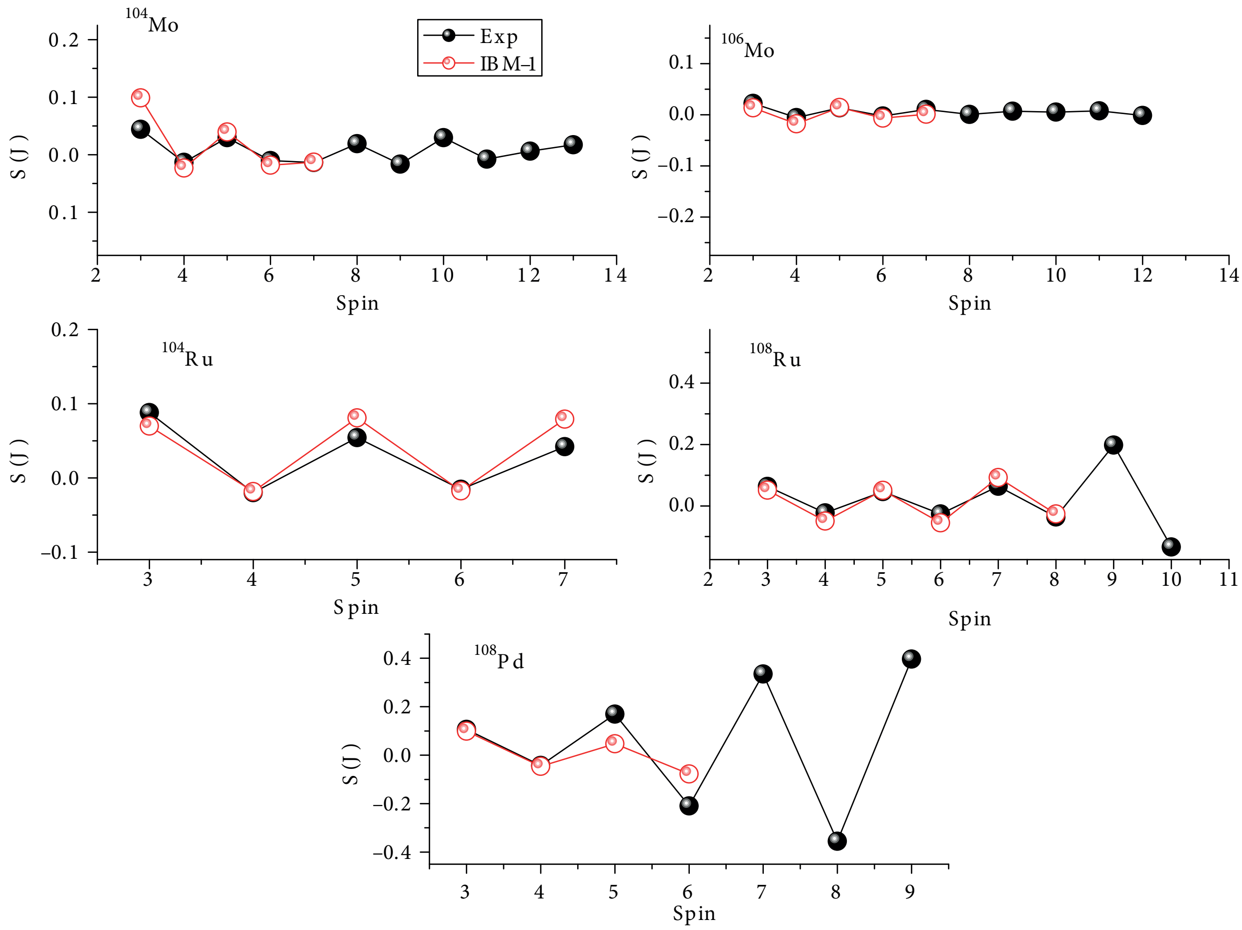

Figure 10. Theoretical (open circle) and experimental (solid circle) odd–even staggering plots in keV for $^{104-106}$Mo, ^{104,108}Ru, and ^{108}Pd nuclei.

3.2. Back bending

The discrete derivatives of the resulting energies with respect to the angular momentum [41] are

$$\hbar\omega = \frac{dE(J)}{dJ} \approx \frac{1}{2}[E(J+2) - E(J)]. \tag{6}$$

Alternatively, the angular velocity can also be defined by using the expression for $E(J)$ provided by symmetric rotor Hamiltonian:

$$E(J) = \frac{J(J+1)}{\Im}. \tag{7}$$

Table 4. The experimental and calculated difference $\triangle E_1$ (keV) and $\triangle E_2$ (keV).

Nuclei	^{94}Mo	^{96}Mo	^{98}Mo	^{100}Mo	^{102}Mo	^{104}Mo	^{106}Mo	^{108}Mo
Exp.$\triangle E_1$	69.0	425	441.2	392.3	195.9	23.9	3.2	3.3
Exp.$\triangle E_2$	510	1206	980.2	599	91.5	83.5	20.1	167.3
Th.$\triangle E_1$	641	500	71.7	26.2	251.2	292.2	175.6	739.7
Th.$\triangle E_2$	14.06	1273	543	448	16.4	109.2	1.4	934
Nuclei	^{94}Ru	^{96}Ru	^{98}Ru	^{100}Ru	^{102}Ru	^{104}Ru	^{106}Ru	^{108}Ru
Exp.$\triangle E_1$	3940.6	133.6	53.3	20.49	56.5	8.9	3.2	24.78
Exp.$\triangle E_2$	5048	286.1	688.6	424.2	534.8	362.0	361.2	174.8
Th.$\triangle E_1$	4650	420.3	19	170.3	124.4	33.6	20.8	55.4
Th.$\triangle E_2$	6171.9	348.7	634	334.1	614.1	305.4	385.3	180.9
Nuclei	^{100}Pd	^{102}Pd	^{104}Pd	^{106}Pd	^{108}Pd	^{110}Pd		
Exp.$\triangle E_1$	106.6	20.6	528.9	516.3	29.9	1588.3		
Exp.$\triangle E_2$	386.6	277.3	614.5	695.2	580.8	1668.4		
Th.$\triangle E_1$	326.8	402.8	212.3	162.2	280.5	1328.6		
Th.$\triangle E_2$	288.2	96.62	827.3	670.8	765.3	1712.9		

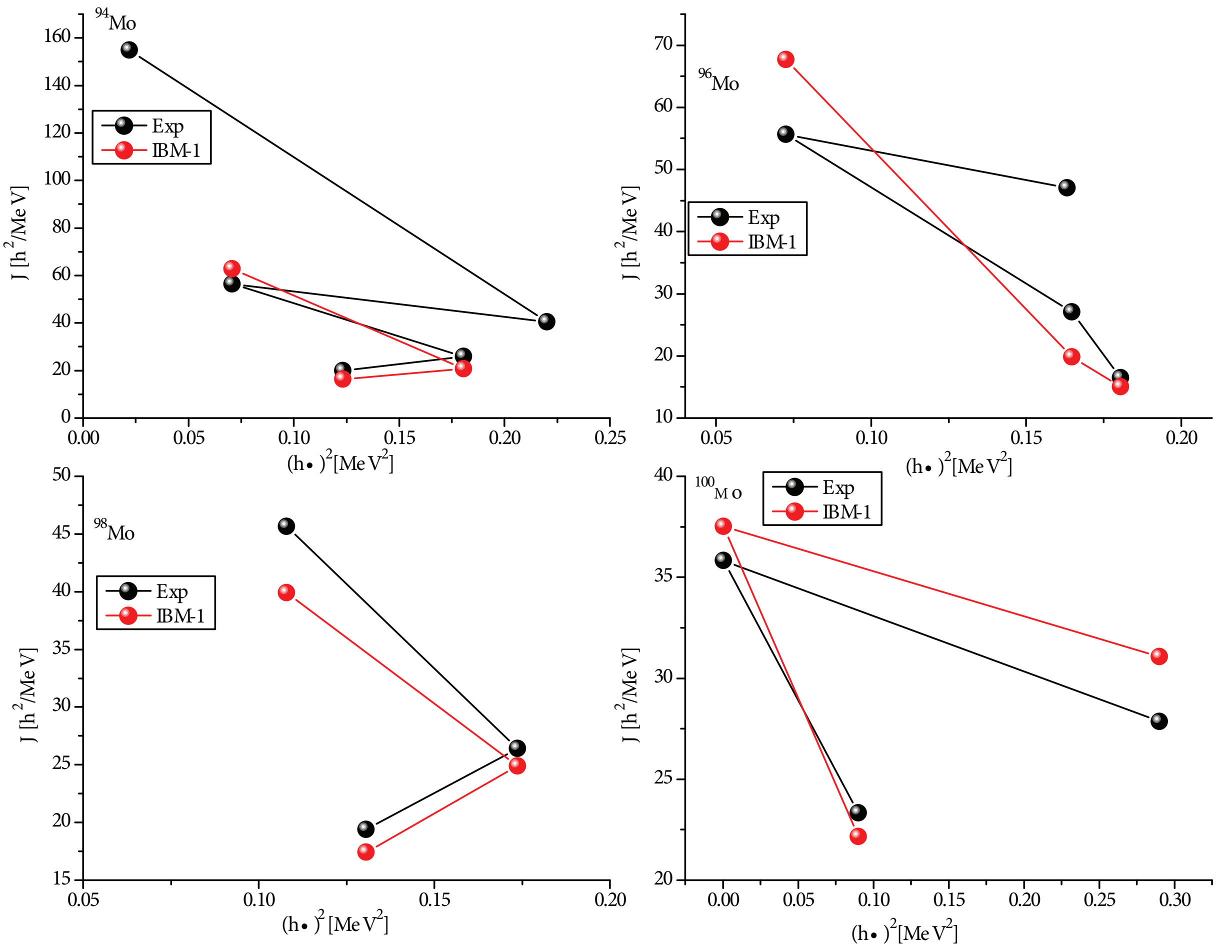

Figure 11. Back bending in $^{94-100}$Mo isotopes.

Then the discrete derivative of this expression yields

$$\hbar\omega(J) = \frac{2J+3}{\Im}, \tag{8}$$

from where one derives a simple expression for the moment of inertia:

$$\Im = \frac{4J+6}{E(J+2)-E(J)} \tag{9}$$

The back bending plot is shown in Figures 11–13 for even–even $^{94-100}$Mo, $^{102-106}$Pd and $^{98-106}$Ru nuclei. The back bending plot is a graph in which moment of inertia versus $(\hbar\omega)^2$ is plotted. The IBM-1 and IBM-2 results and experimental data are usually compared in terms of these plots. The back bending is associated with the breaking of the first neutron $(h_{11/2})^2$ pair. In Figures 11 and 12, $^{94-100}$Mo and $^{102-106}$Pd isotopes show backbending effect at $J = 8^+$. Similarly in Figure 13, $^{98-106}$Ru isotopes also show this backbending effect below $J = 12^+$. It means there is a band crossing and this is also confirmed by calculating the staggering effect of these isotopes. A disturbance of the angular band structure has been observed not only in the moment of inertia but also in the decay properties.

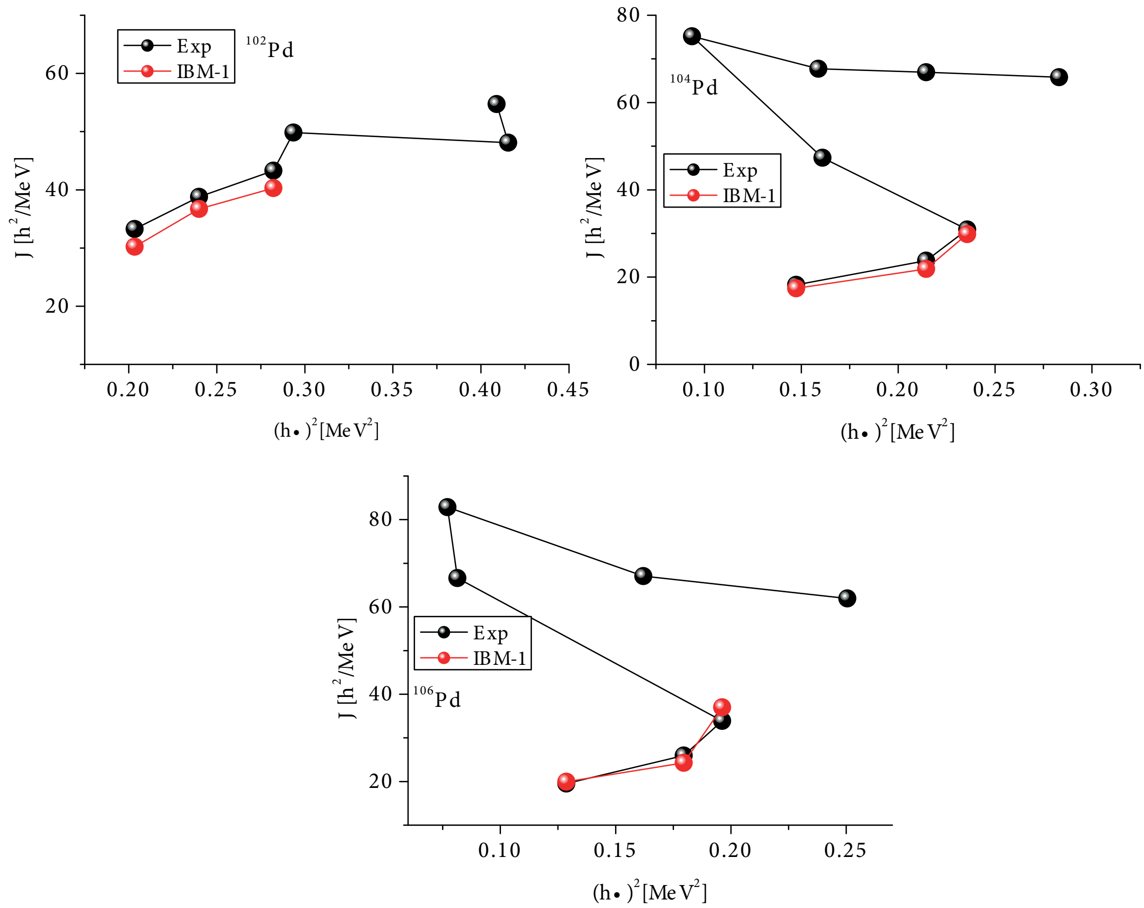

Figure 12. Back bending in $^{102-106}$Pd isotopes.

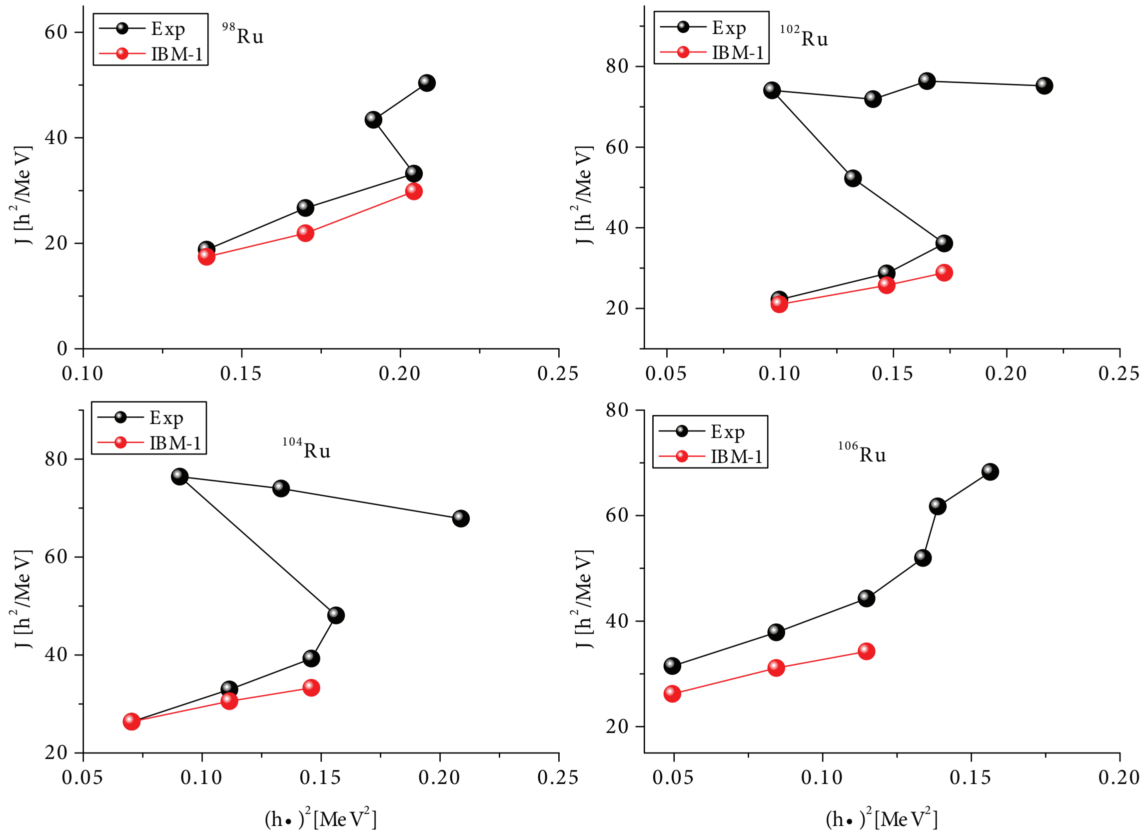

Figure 13. Back bending in $^{98,102-106}$Ru isotopes.

4. Conclusion

The results of this work show that the IBM-1 provides a good description of even–even Mo, Ru, and Pd isotopes of the nuclei. The results of our phenomenological analysis indicate that the interacting boson model can reproduce a considerable quantity of experimental data. It gives useful indications where data are lacking. One observes the transitions between 3 limit symmetries of the model, corresponding to different nuclear shapes along the isotopes chain, collective levels, and electromagnetic transitions between them. The calculated level structure of the $^{102-108}$Mo isotopes in empirical IBM-1 provides fairly good energy fits for the g-, γ-, and β-band, while the moment of inertia related to $E(2_1^+)$, the $B(E2; 2_1 \rightarrow 0_1)$ and the quadrupole moment and energy ratio $R_{4/2}$ do correspond to the deformed nuclei. The shape transition predicted by this study is consistent with the spectroscopic data for these nuclei. $^{102-108}$Ru are the typical examples of the isotopes that exhibit a smooth phase transition from vibrational nuclei to the γ-soft nuclei. The predictions show that $^{102-108}$Ru isotopes are lined up along the SU(5)–O(6) side of the IBM triangle. In the above discussion we also observed the back bending and odd–even staggering effect in the gamma-bands.

As seen in Table 2, estimated B(E2) transitions are mostly in agreement with the IBM-2 and experimental values. Table 3 is devoted to the description of the triaxial nuclei. In the table we calculate the most distinctive signature of the triaxial rigid rotor relating the energies of the 3 particular states. The deviations obtained suggested that some isotopes have a near triaxial nature. Bending for Mo and Pd isotopes has been observed at angular momentum 8^+ and bending for Ru isotopes observed at angular momentum 12^+.

In view of the growing pursuit in this kind of theoretical interest, it is assumed that a new study investigating the properties of neutron rich full isotopic mass chains around $A \cong 100$ mass region will also be carried out.

References

[1] Arima, A.; Iachello, F. *Phys. Rev. Lett.* **1975**, *35*, 1069–1072.

[2] Arima, A.; Iachello, F. *Ann. Phys. (NY)* **1978**, *111*, 201–238.

[3] Iachello, F.; Arima, A. *Interacting Boson Model*; Cambridge University Press, Cambridge, 1987.

[4] Arima, A.; Iachello, F. *Phys. Rev. Lett.* **1978**, *40*, 385–387.

[5] Cizewski, J. A.; Casten, R. F.; Smith, G. J.; Stelts, M. L.; Kane, W. R.; Bğrner, H. G.; Davidson, W. F. *Phys. Rev. Lett.* **1978**, *40*, 167–170.

[6] Scholten, O.; Iachello, F.; Arima, A. *Ann. Phys. (N.Y)* **1978**, *115*, 325–366.

[7] Warner, D. D.; Casten, R. F.; Davidson, W. F. *Phys. Rev. Lett.*, **1980** , *45*, 1761–1765.

[8] Casten R. F. *Interacting Bose-Fermi Systems in Nuclei*, Iachello F. Ed.; Plenum, New York, 1981, 1.

[9] Ginocchio, J. N.; Kirson, M. W. *Phys. Rev. Lett.* **1980**, *44*, 1744–1747.

[10] Dieperink, A. E. L.; Scholten, O.; Iachello, F. *Phys. Rev. Lett.*, **1980**, *44*, 1747–1750.

[11] McCutchen, E. A.; Zamfir, N. V.; Casten, R. F. *Phys. Rev. C* **2004**, *69*, 064306.

[12] McCutchen, E. A.; Zamfir, N. V. *Phys. Rev. C* **2005**, *71*, 054306.

[13] Iachello, F. *Phys. Rev. Lett.* **2001**, *87*, 052502.

[14] Raduta, A. A.; Buganu, P. *Phys. Rev. C* **2011**, *83*, 034313.

[15] Iachello, F. *Phys. Rev. Lett.* **2000**, *85*, 3580–3583.

[16] Casten, R. F.; Zamfir, N. V. *Phys. Rev. Lett.* **2000**, *85*, 3584–3586.

[17] Casten, R. F.; Zamfir, N. V. *Phys. Rev. Lett.* **2001** , *87*, 052503.

[18] Bizzeti, P. G.; Bizzeti-Sona, A. M. *Phys. Rev. C* **2002**, *66*, 031301(R).

[19] Bizzeti, P. G.; Bizzeti-Sona, A. M. *Phys. Rev. C* **2010**, *81*, 034320.

[20] Iachello, F. *Phys. Rev. Lett.* **2003**, *91*, 132502.

[21] Bonatsos, D.; Lenis, D.; Petrellis, D.; Terziev, P. A. *Phys. Lett. B* **2004** , *588*, 172–179.

[22] Minkov, N.; Drenska, S. B.; Raychev, P.P.; Roussev, R. P.; Bonatsos, D. *Phys. Rev. C* **1997**, *55*, 2345–2360.

[23] Minkov, N.; Drenska, S. B.; Raychev, P.P.; Roussev, R. P.; Bonatsos, D. *Phys. Rev. C* **2000**, *61*, 064301.

[24] Singh, A. J.; Raina, P. K. *Phys. Rev. C* **1996**, *53*, 1258–1265.

[25] Scholten, O. *Computer Program PHINT*; University of Groningen, The Netherlands, 1976.

[26] Casten, R. F.; Warner, D. D. *Rev. Mod. Phys.* **1988**, *60*, 389–469.

[27] Warner, D. D.; Casten, R. F. *Phys. Rev. C* **1983**, *28*, 1798–1806.

[28] Alaga, A.; Aldern, K.; Bohr, A.; Mottelson, B. R. *Dan. Mat, Fys. Medd.* **1955**, *29*, 9.

[29] Bohr, A.; Mottelson, B. R. *Nuclear Structure*; Benjamin, New York, II, 1975.

[30] von Brentano, P.; Zamfir, N. V.; Casten, R. F. *Phys. Rev. C* **2007**, *76*, 024306.

[31] http://www.nndc.bnl.gov.

[32] Schulz, N. In *Proc. Int. Conference on Properties of Fission and Neutron Rich Nuclei*, Sambel Island, Nov. 1997; Hamilton, J. H.; Ramayya, A. V. Eds.; Singapore, World Scientific, p. 260.

[33] Frank, A.; Van Isacker, P.; Warner, D. D. *Phys. Lett. B* **1987**, *197*, 474–478.

[34] Frank, A. *Phys. Rev. Lett.* **1988**, *60*, 2099–2099.

[35] Troltenier, D.; Maruhm, J. A.; Greiner, W.; Velazquez Aguilar, V.; Hess, P. O.; Hamilton, J. H. *Z. Phys. A* **1991**, *338*, 261–270.

[36] Federman, P.; Pittel, S. *Phys. Lett. B* **1977**, *69*, 385–388.

[37] Nair, C. K.; Ansari, A.; Satpathy, L. *Phys. Lett. B* **1977**, *71*, 257–258.

[38] Bonatsos, D. *Phys. Lett. B* **1988**, *200*, 1–7.

[39] Lalkovski, S.; Minkov, N. *J. Phys. G; Nucl. Part. Phys.* **2005**, *31*, 427–444.

[40] Wilets, L.; Jean, M. *Phy. Rev.* **1956**, *102*, 788–796.

[41] Raduta, A. A.; Budaca, R. *Phys. Rev. C* **2011**, *84*, 044323.

[42] Jin-Fu, Z.; AL-Khudair, H. F.; Gui-Lu, L.; Sheng-Jiang, Z.; Dong, R. *Commun. Theor. Phys. (Beijing, China)* **2002**, *37*, 335–340.

[43] Inci, I.; Turkan, N. *Turk. J. Phys.* **2006**, *30*, 493–502.

[44] Inci, I.; Turkan, N. *Turk. J. Phys.* **2006**, *30*, 503-512.

[45] Kim, K. H.; Gelberg, A.; Mizusaki, T.; Otsuka, T.; von Brentano, P. *Nuclear Physics A* **1996**, *604*, 163–182.

[46] Long, G. L.; Liu, Y. X.; Sun, H. Z. *J. Phys. G: Nucl. Part. Phys.* **1990**, *16*, 813–822.